

Supporting Information

E-H Bond Activation Reactions (E = H, C, Si, Ge) at Ru: Terminal Phosphides, Silylenes, and Germylenes

*Ayumi Takaoka, Arjun Mendiratta, Jonas C. Peters**

Massachusetts Institute of Technology

jcpeters@mit.edu

Contents

Figure S1. Fully labeled diagram of **9**.

Figure S2. ^1H - ^{29}Si HSQC spectrum of **9**.

Table S1. Kinetic data for Eyring plot for the decay of **5**.

Figure S3. Eyring plot for the decay of **5**.

Figure S4. Typical decay behavior of **5** vs $d_{30}\text{-[SiP}^{\text{Ph}}\text{]}_3\text{Ru(PPh}_2\text{)}$ at 35°C.

Figure S5. NMR spectra for **4**.

Figure S6. NMR spectra for **5**.

Figure S7. NMR spectra for **8**.

Figure S8. NMR spectra for **9**.

Figure S9. NMR spectra for **10b**.

Figure S10. NMR spectra for **12**.

Figure S11. NMR spectra for **13**.

Figure S1. Fully labeled diagram of $[\text{SiP}^{\text{Ph}}_3]\text{Ru}(\text{H})(\eta^2\text{-H}_2\text{SiPh}_2)$ (**9**) and co-crystallized solvent.

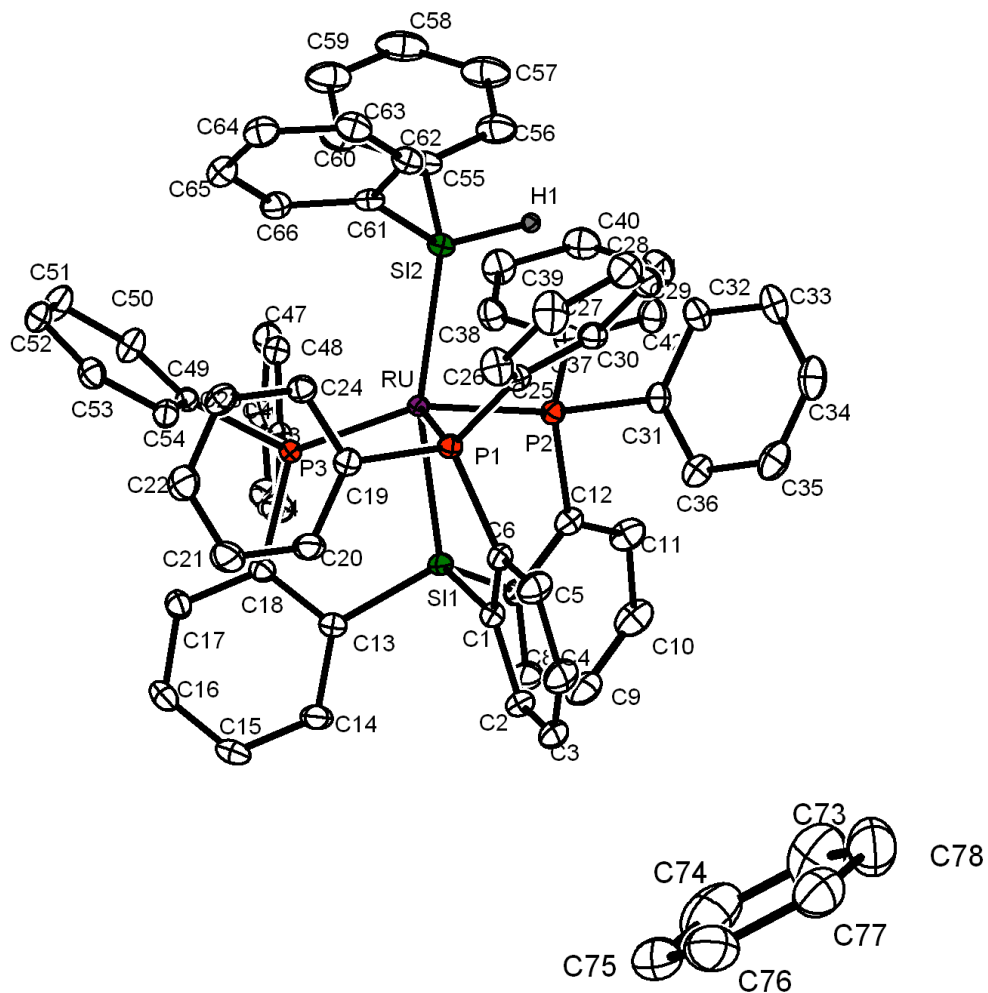


Figure S2. ^1H - ^{29}Si HSQC spectrum of **13** of upfield peak in d^8 -THF.

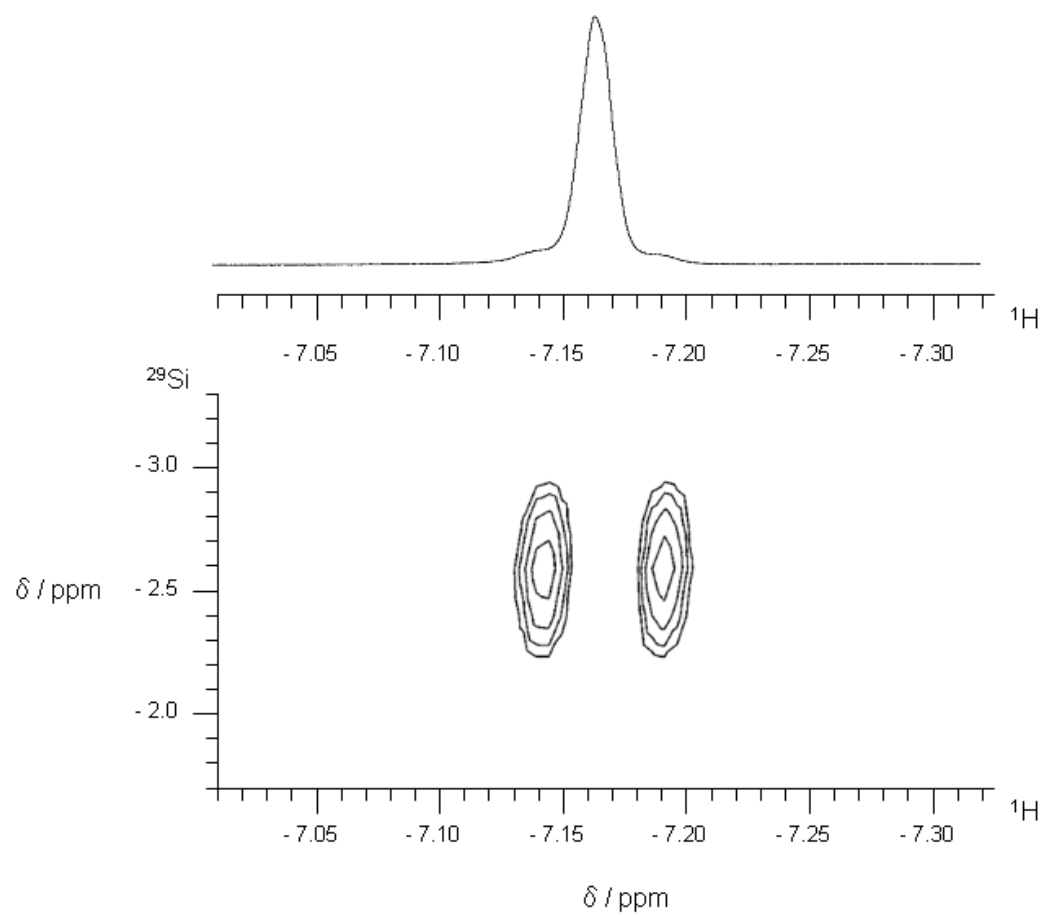


Table S1. Kinetic data for Eyring plot.

T(K)	rate constant(/hr)
298.2	0.0164(4)
308.2	0.0463(15)
318.2	0.138(4)
328.2	0.393(17)

Figure S3. Eyring plot for the decay of **5**.

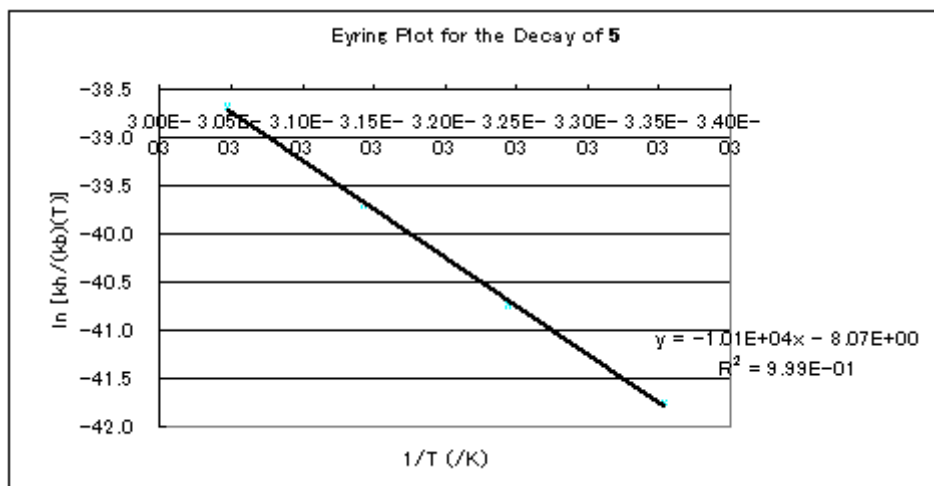
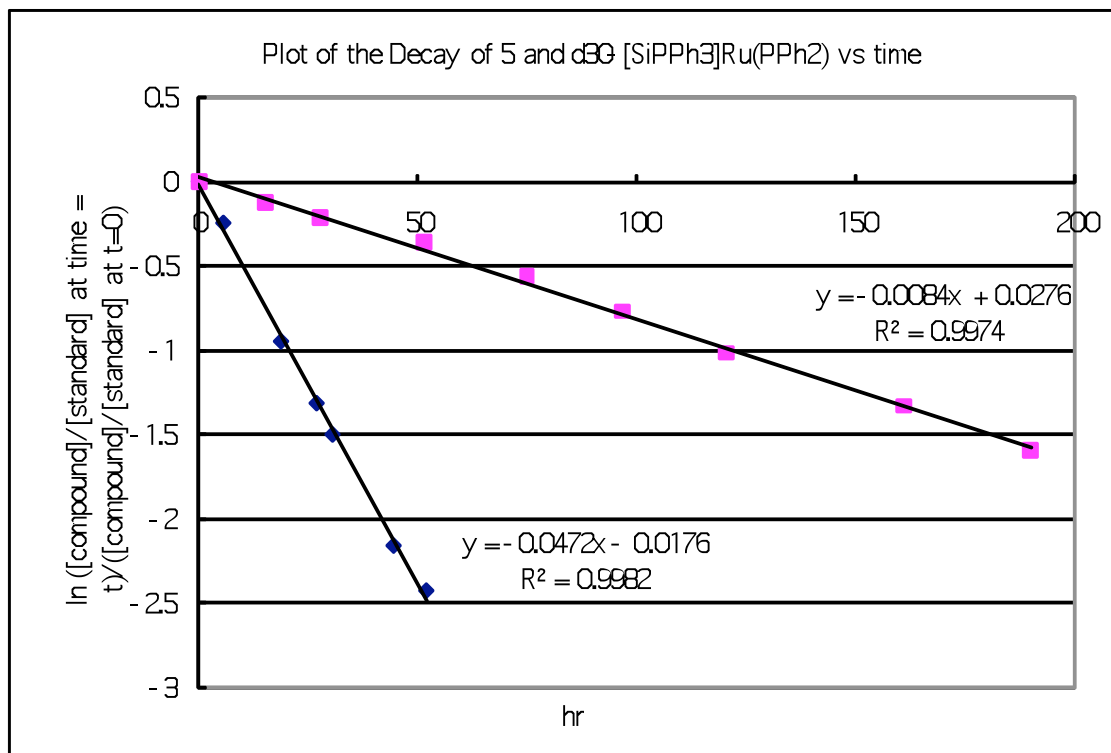


Figure S4. Typical decay behavior of **5** vs d_{30} -[SiP^{Ph}₃]Ru(PPh₂) at 35°C.

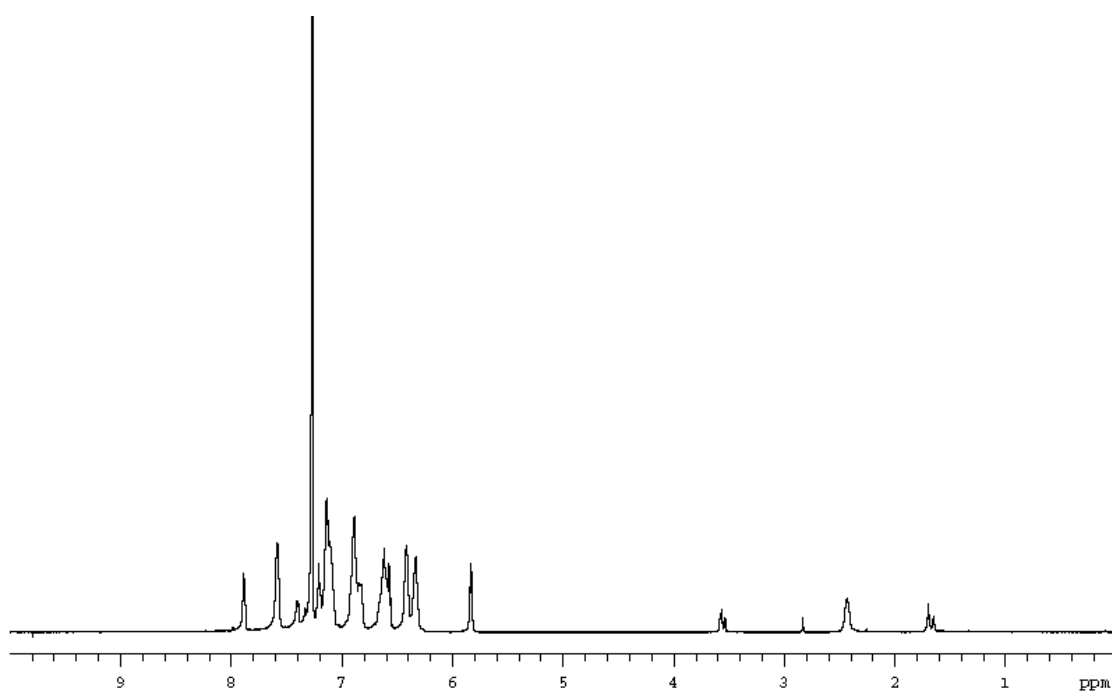


Blue: **5**

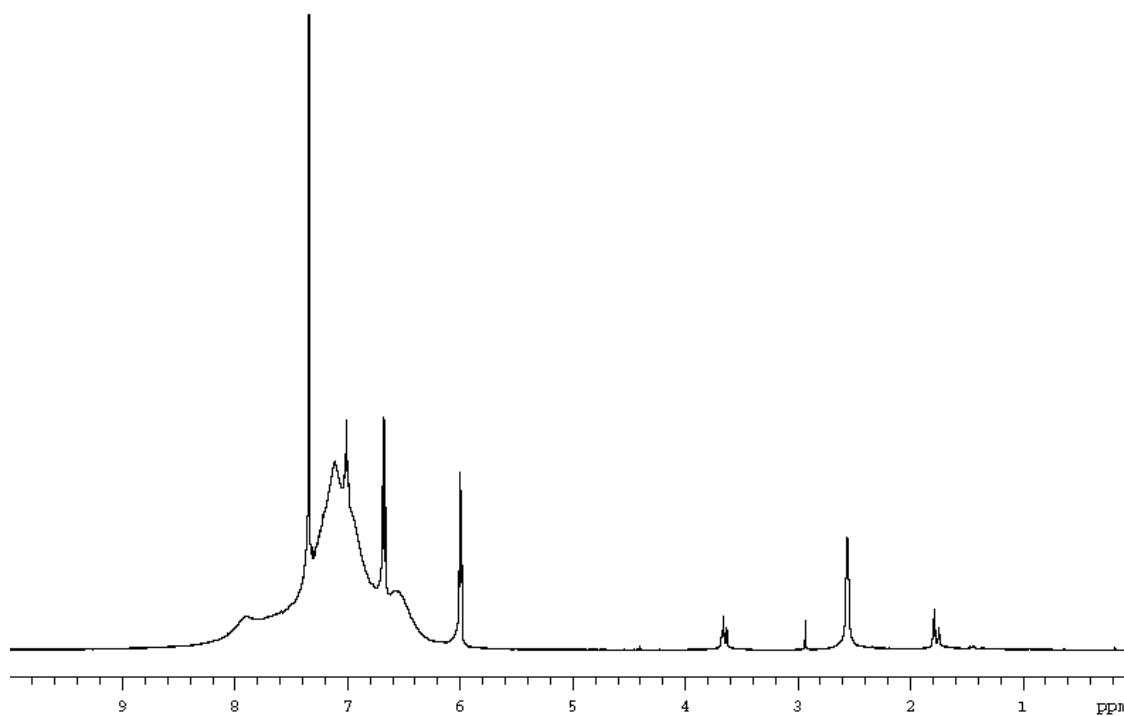
Pink: d_{30} -[SiP^{Ph}₃]Ru(PPh₂)

Figure S5. NMR spectra for **4**.

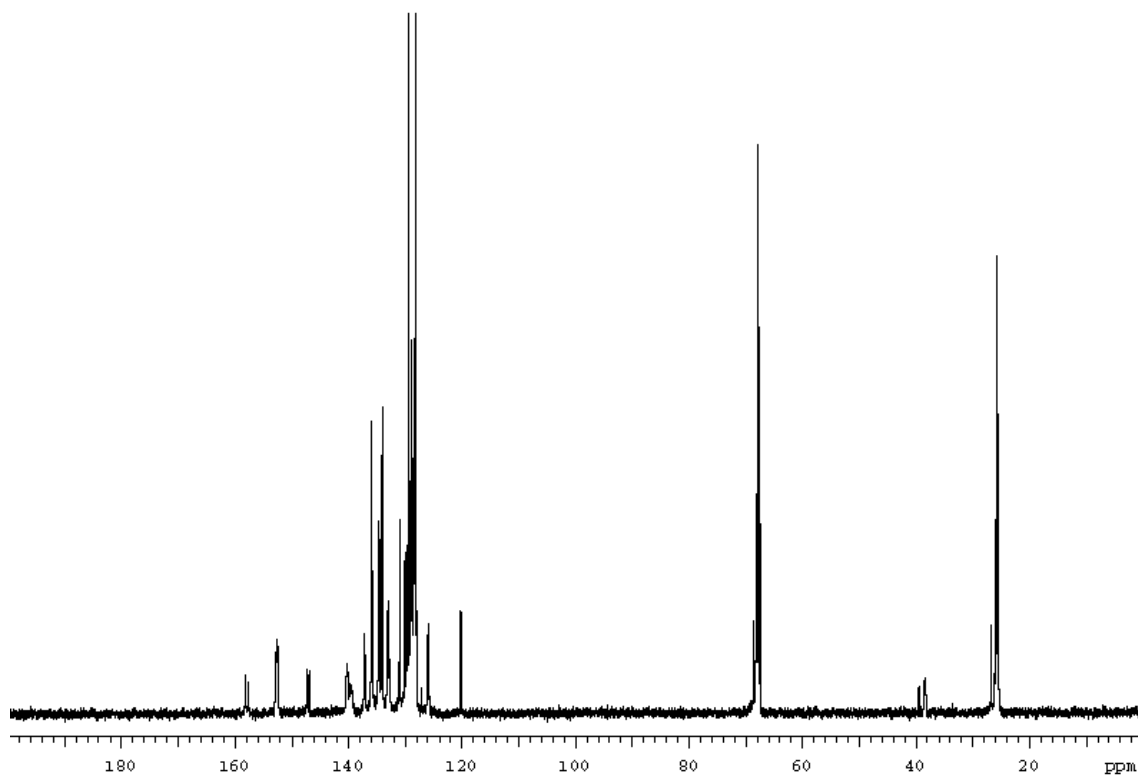
^1H at $-20\text{ }^\circ\text{C}$ in d_8 -THF.



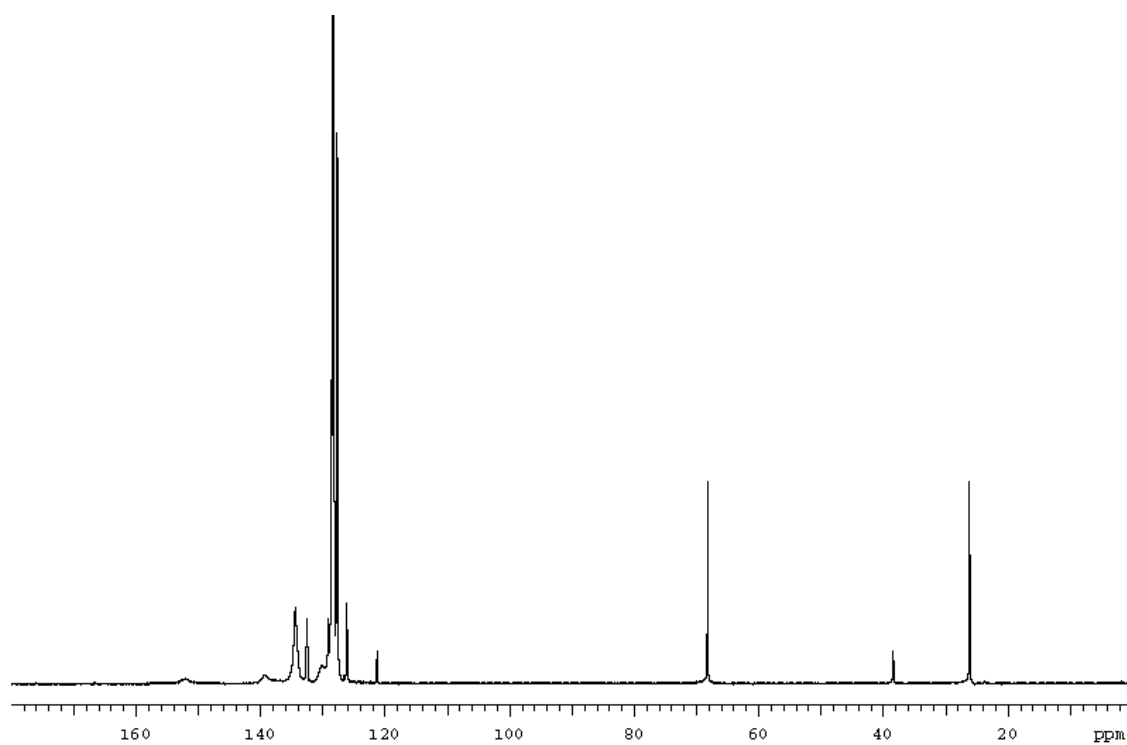
^1H at RT in d_8 -THF.



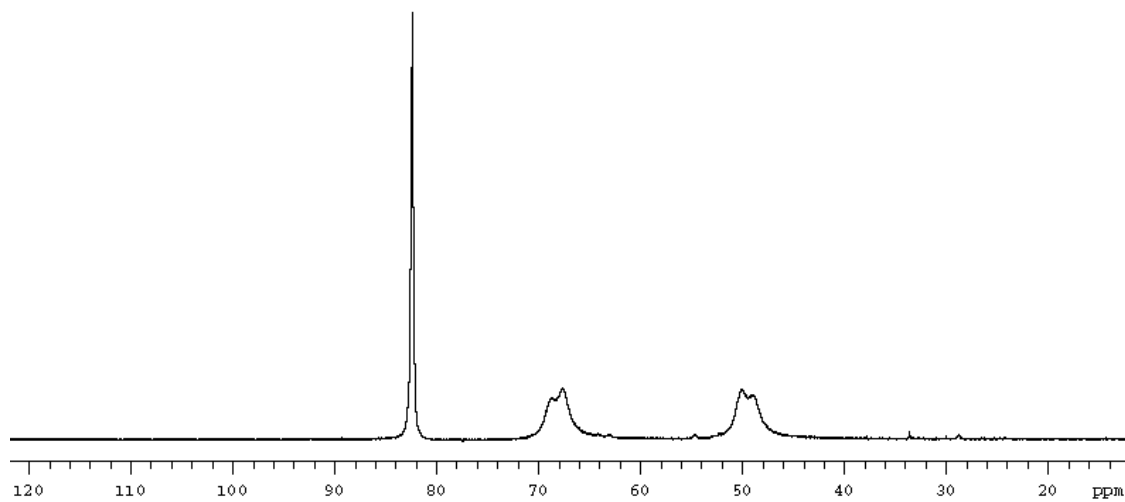
$^{13}\text{C}\{^1\text{H}\}$ at $-20\text{ }^\circ\text{C}$ in $d_8\text{-THF}$.



$^{13}\text{C}\{^1\text{H}\}$ at RT in C_6D_6 .



$^{31}\text{P}\{^1\text{H}\}$ at $-80\text{ }^\circ\text{C}$ in d_8 -THF.



$^{31}\text{P}\{^1\text{H}\}$ at RT in d_8 -THF.

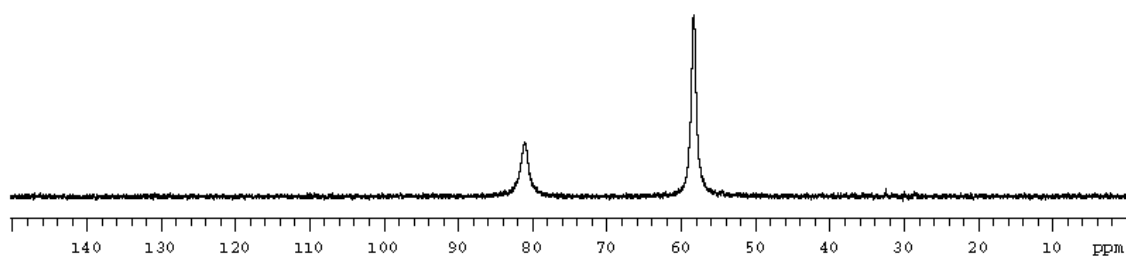
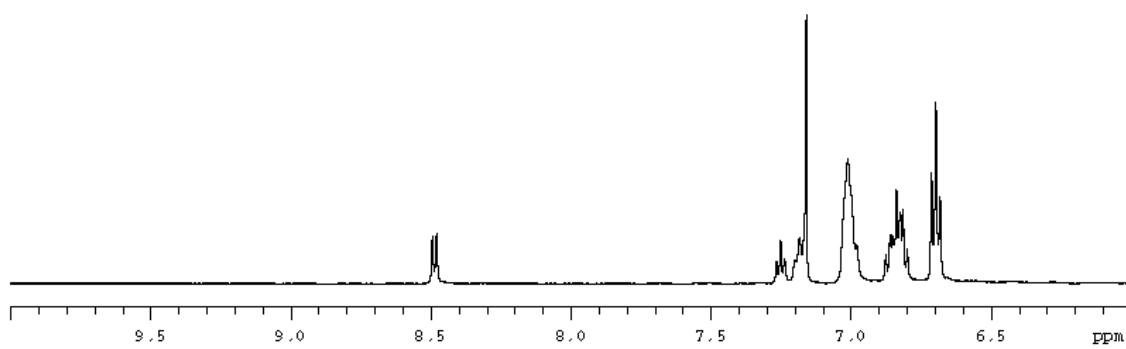
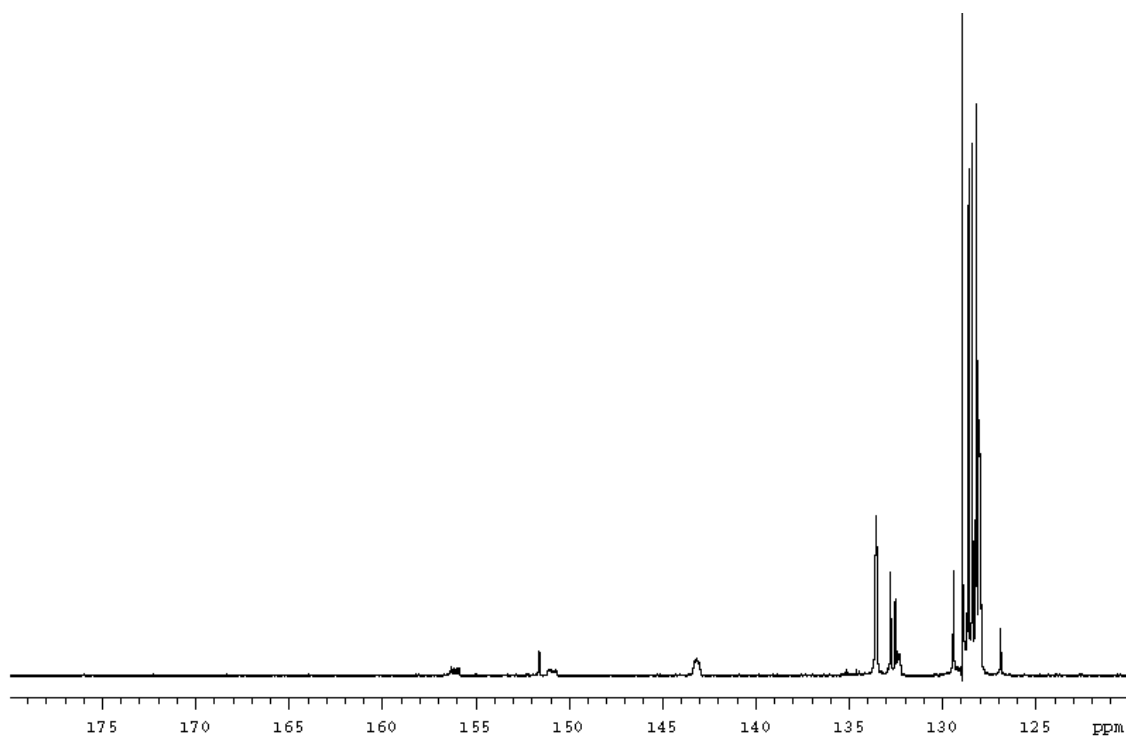


Figure S6. NMR spectra for **5**.

^1H at RT in C_6D_6 .



$^{13}\text{C}\{^1\text{H}\}$ at RT in C_6D_6 .



$^{31}\text{P}\{^1\text{H}\}$ at RT in C_6D_6 .

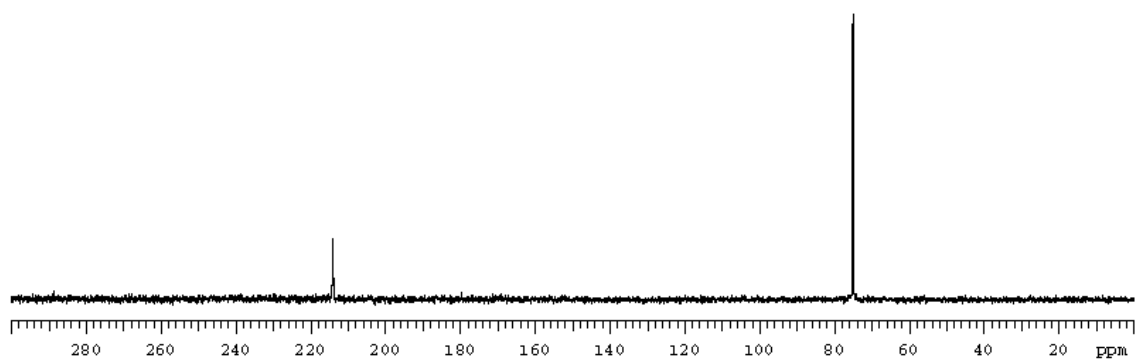
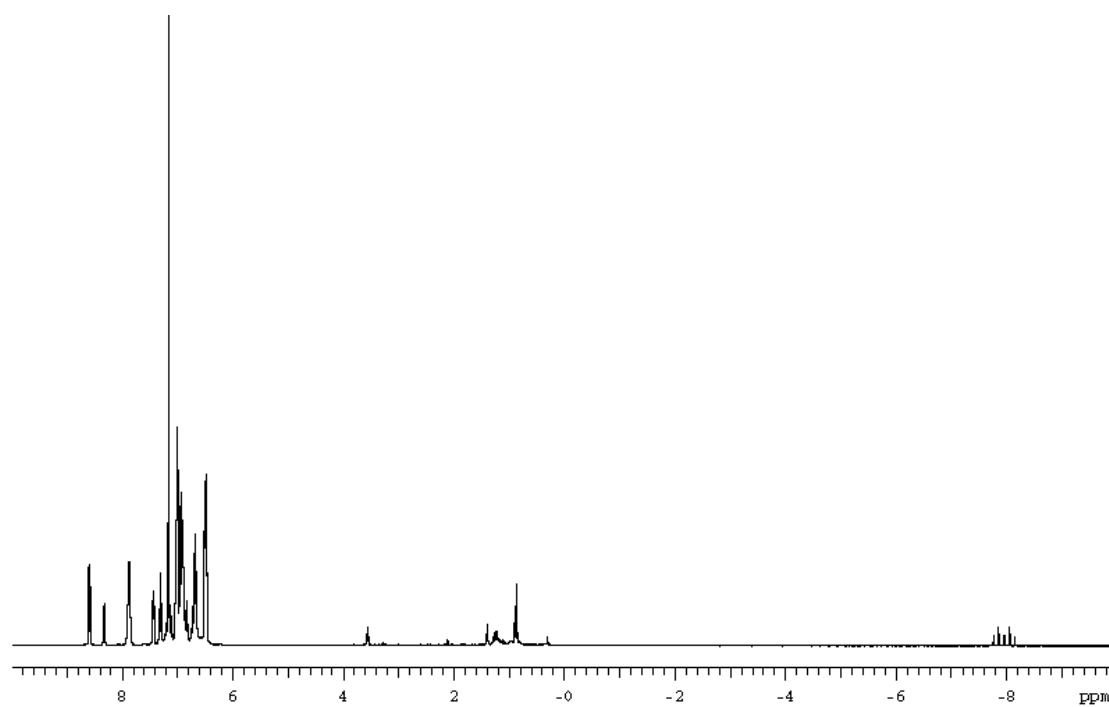
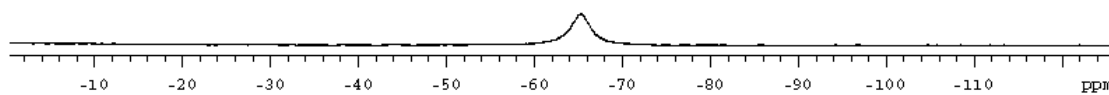


Figure S7. NMR spectra for **8**.

^1H at RT in C_6D_6 .



$^{15}\text{N}\{^1\text{H}\}$ at RT in C_6D_6 .



$^{31}\text{P}\{^1\text{H}\}$ at RT in C_6D_6 .

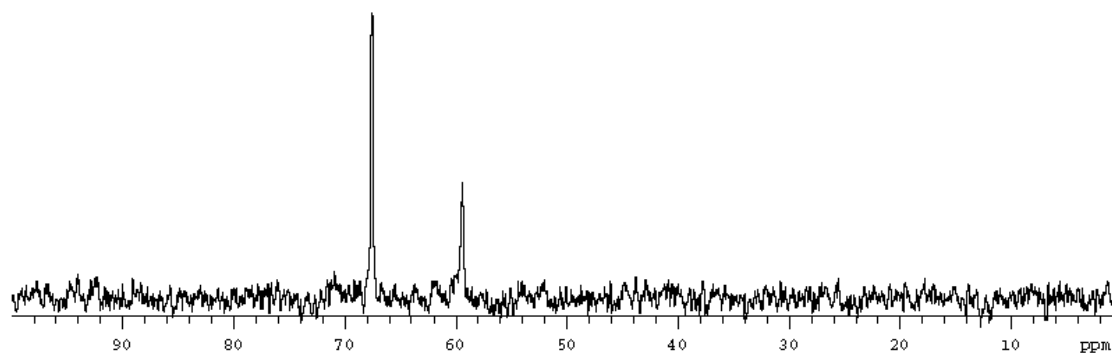
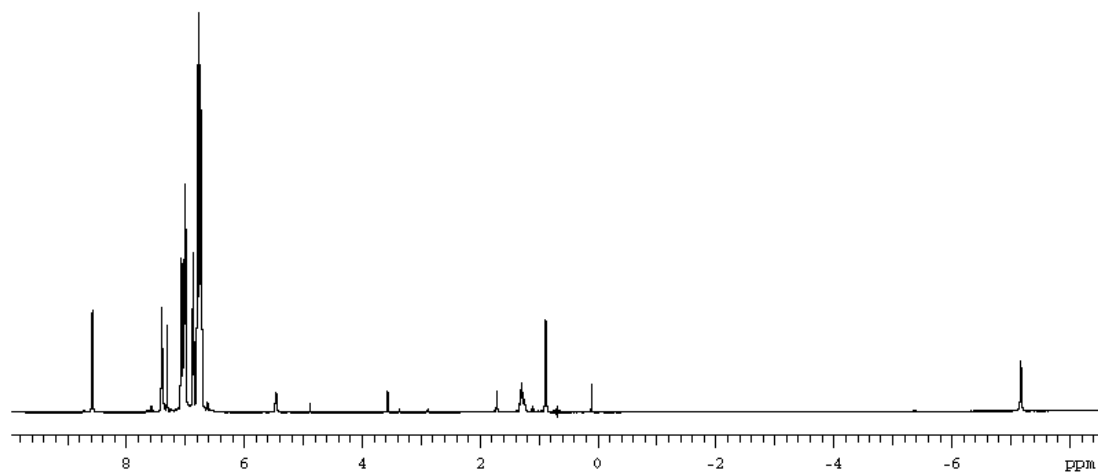
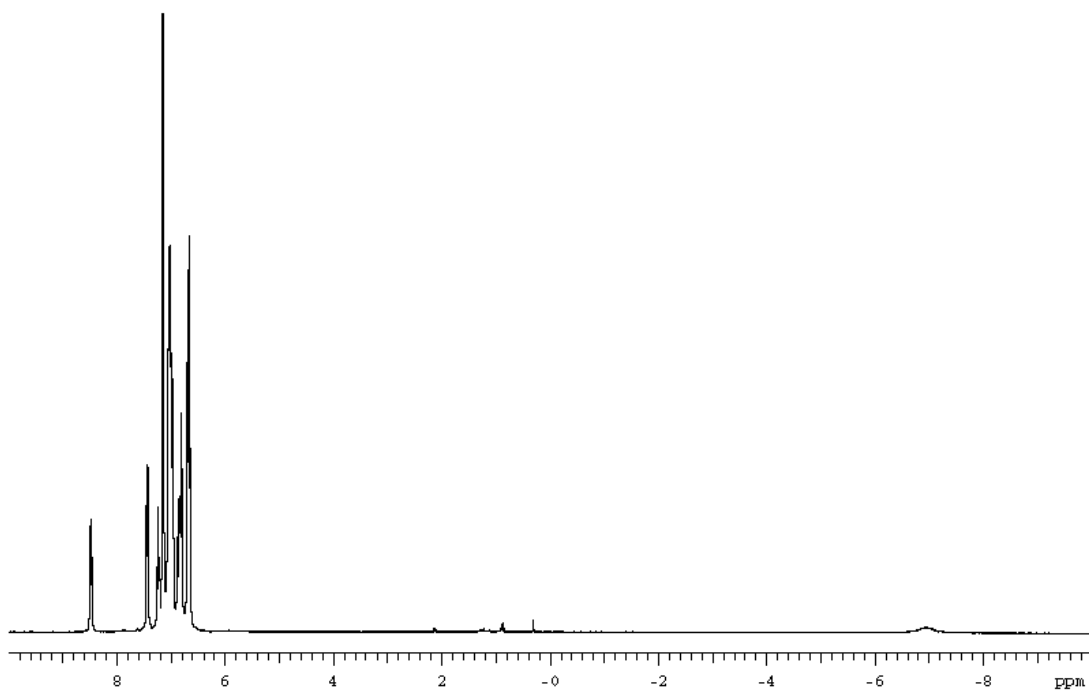


Figure S8. NMR spectra for **9**.

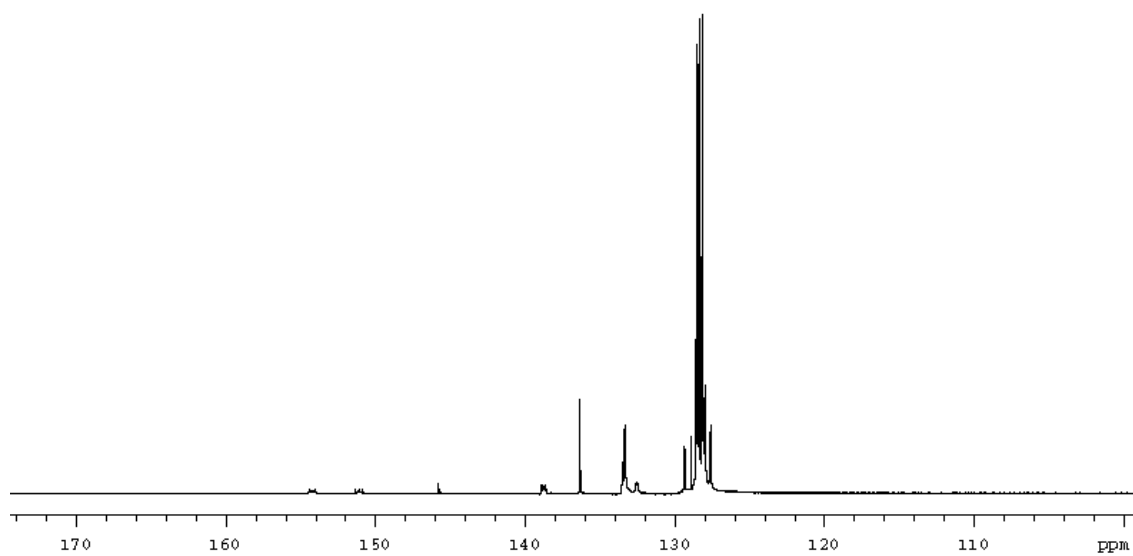
^1H at $-20\text{ }^\circ\text{C}$ in d_8 -THF.



^1H at RT in C_6D_6 .



$^{13}\text{C}\{^1\text{H}\}$ at RT in C_6D_6 .



$^{31}\text{P}\{^1\text{H}\}$ at RT in C_6D_6 .

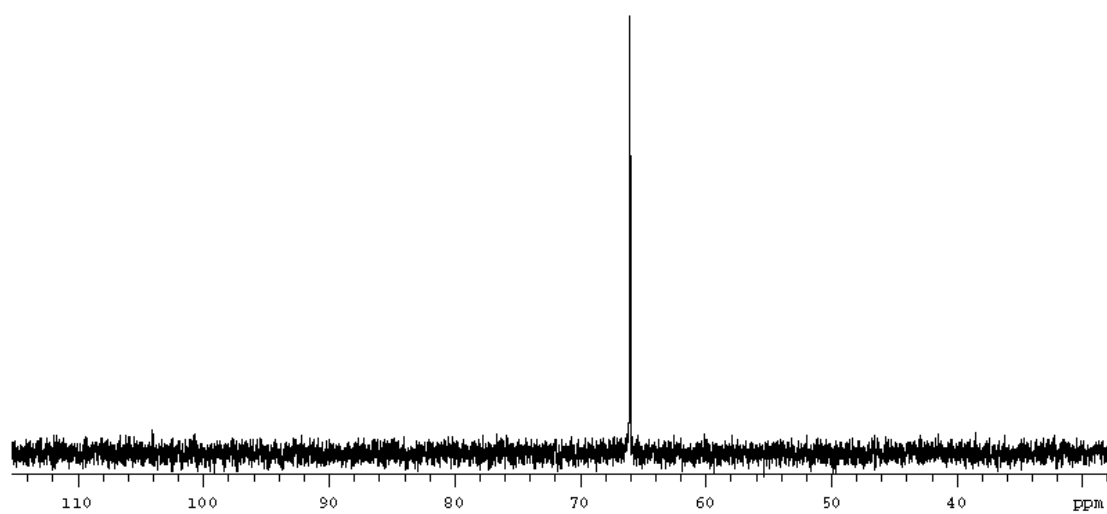
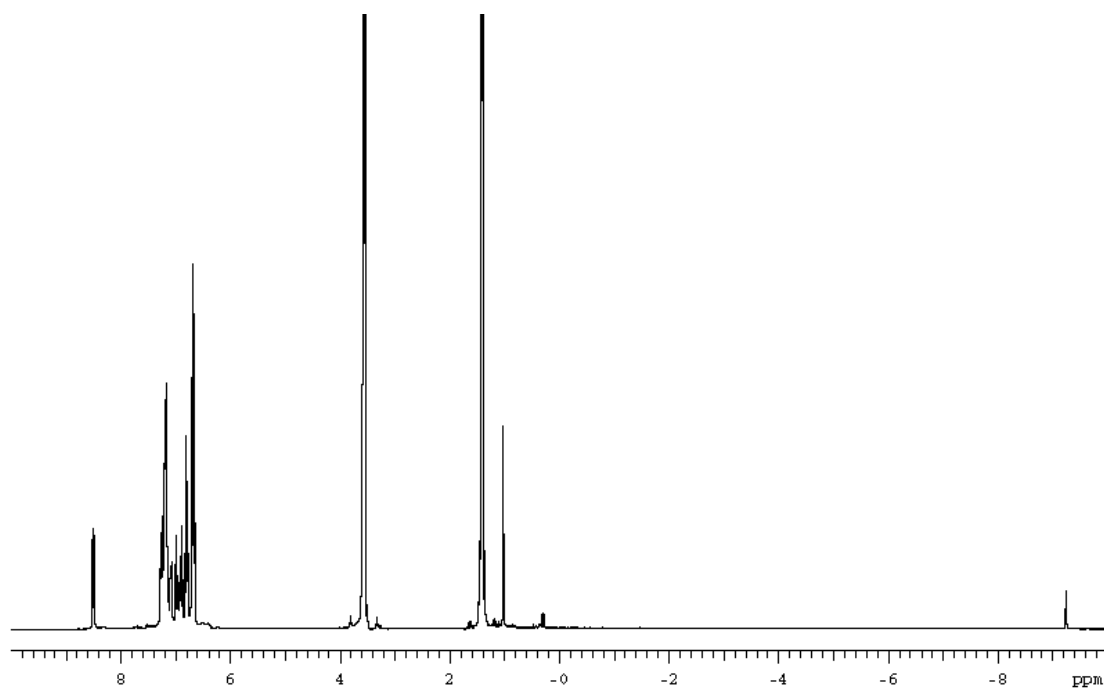
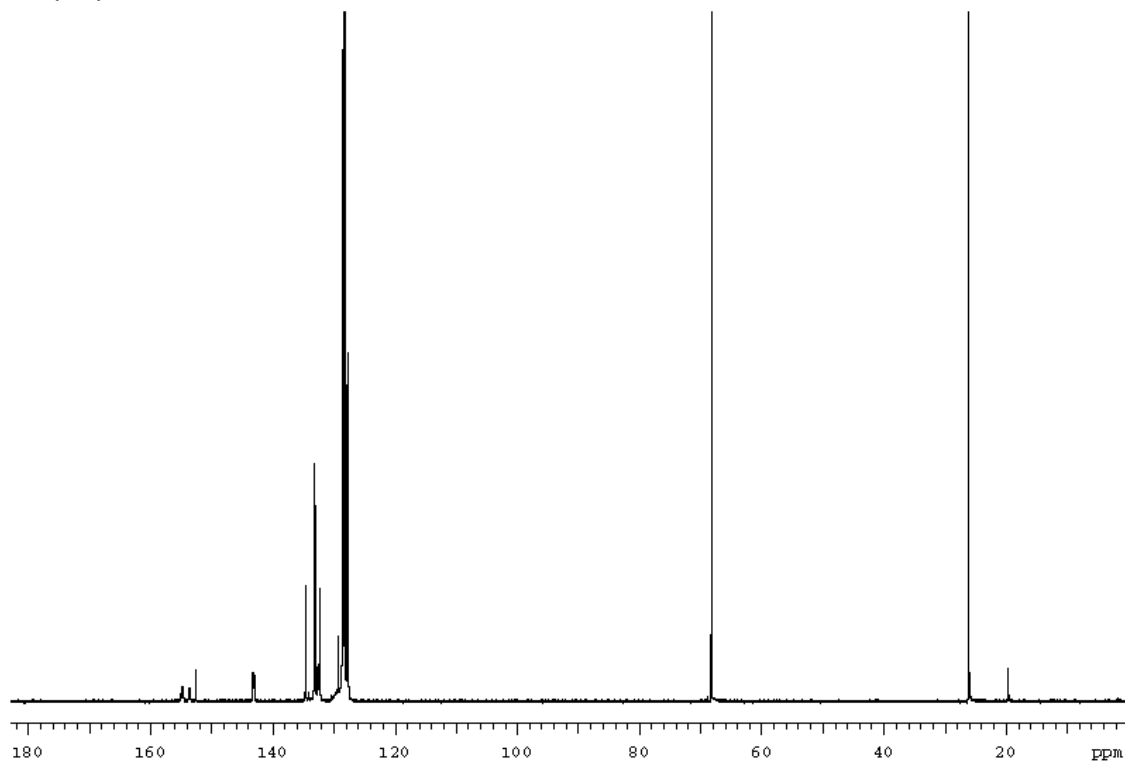


Figure S9. NMR spectra for **10b**.

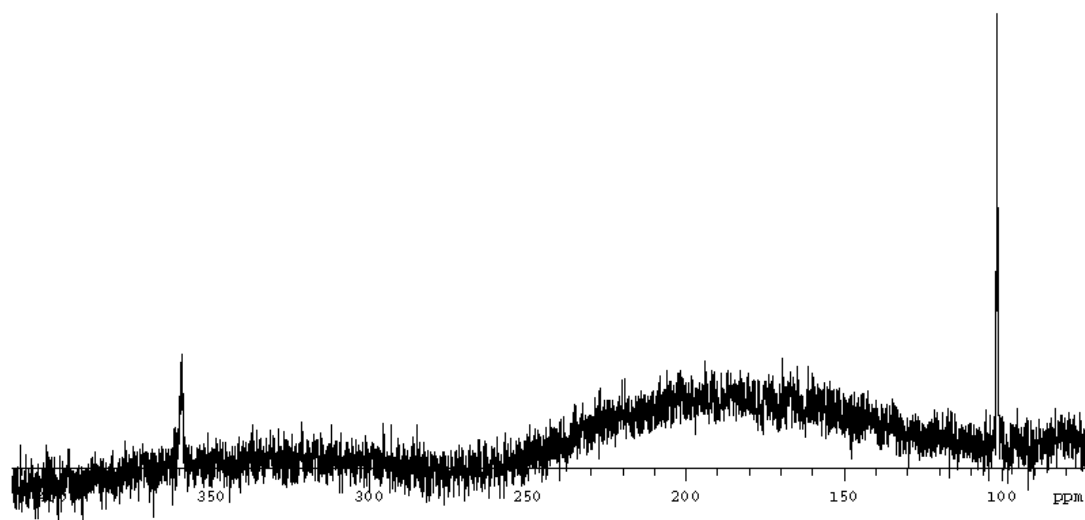
^1H at RT in C_6D_6 .



$^{13}\text{C}\{^1\text{H}\}$ at RT in C_6D_6 .



$^{29}\text{Si}\{^1\text{H}\}$ at RT in C_6D_6 .



$^{31}\text{P}\{^1\text{H}\}$ at RT in C_6D_6 .

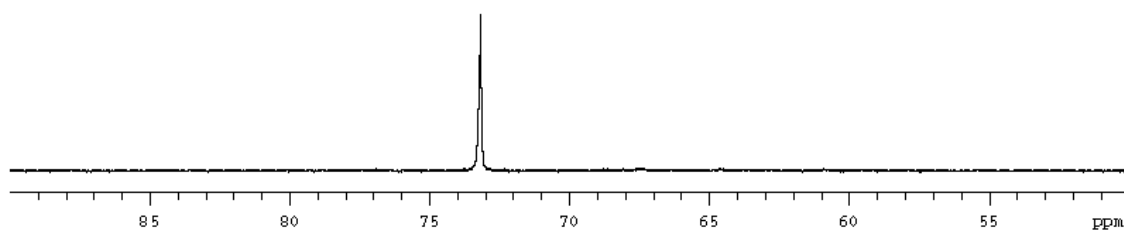
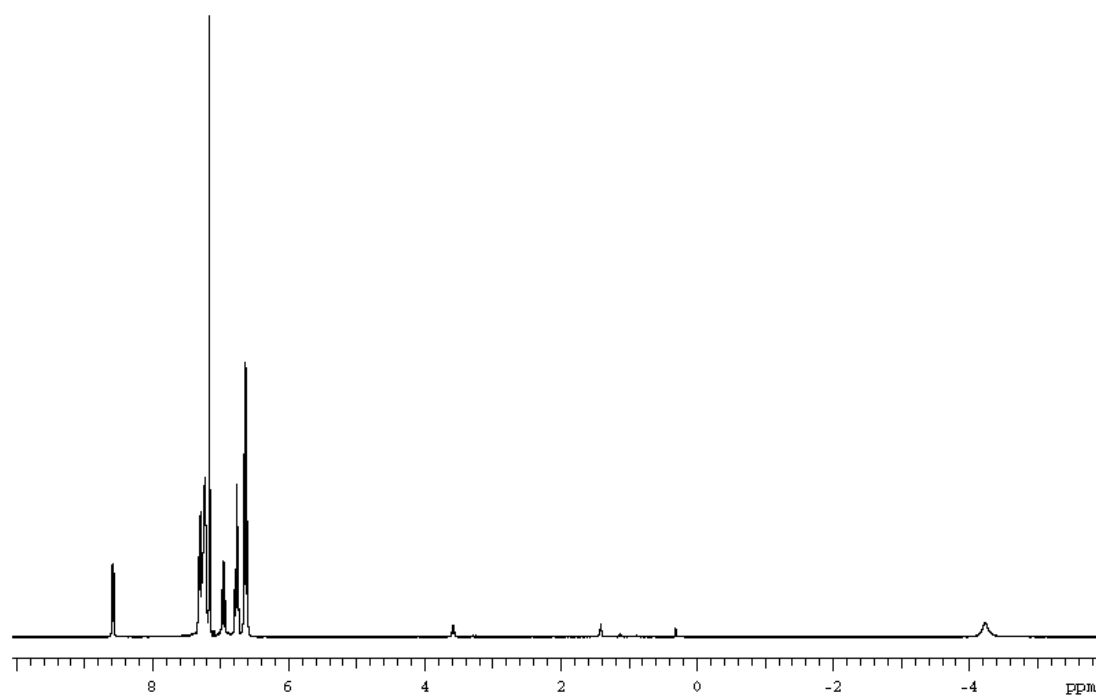


Figure S10. NMR spectra for **12**.

^1H at RT in C_6D_6 .



$^{31}\text{P}\{^1\text{H}\}$ at RT in C_6D_6 .

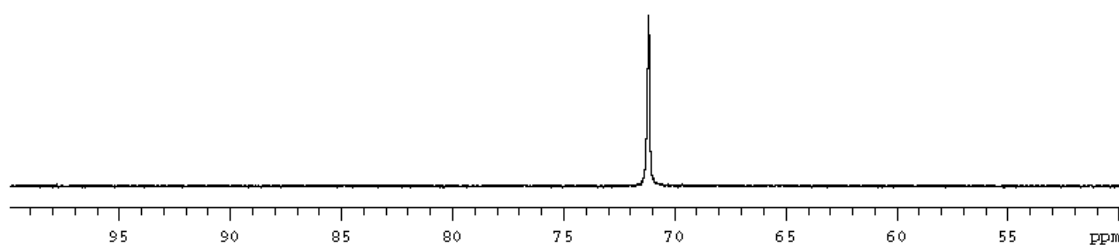
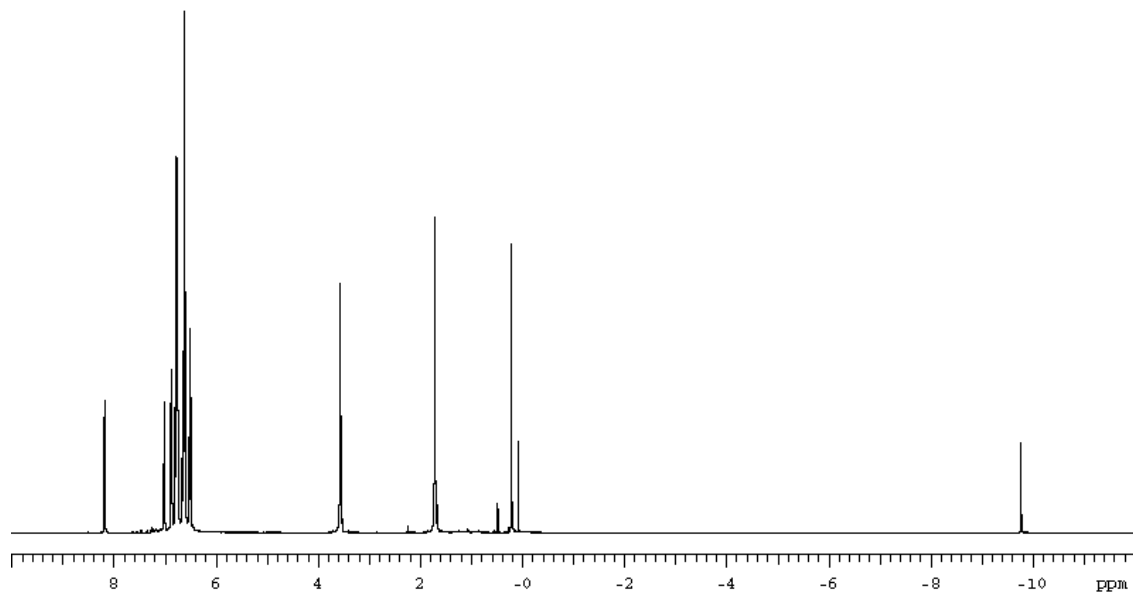
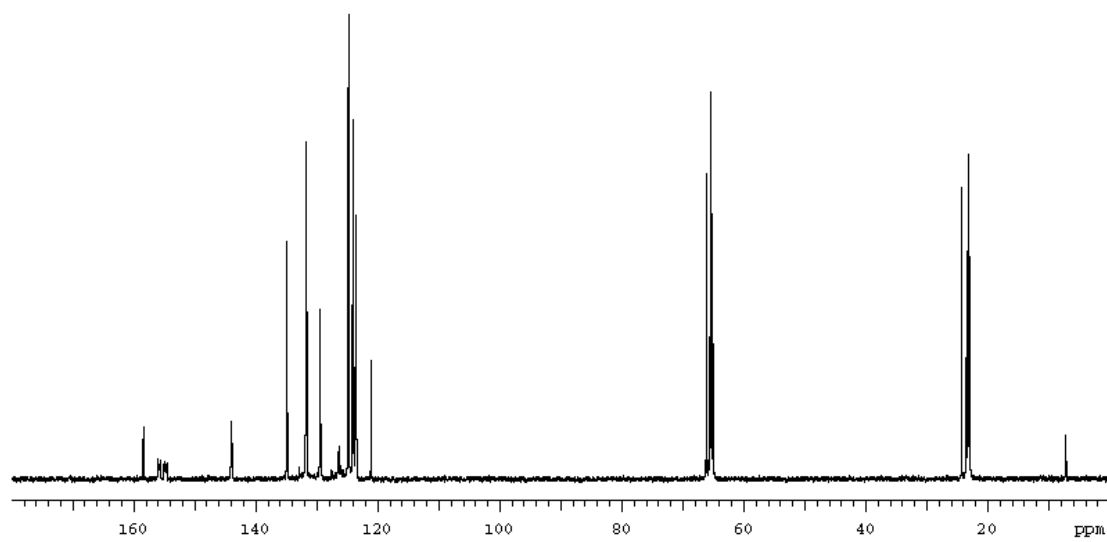


Figure S11. NMR spectra for **13**.

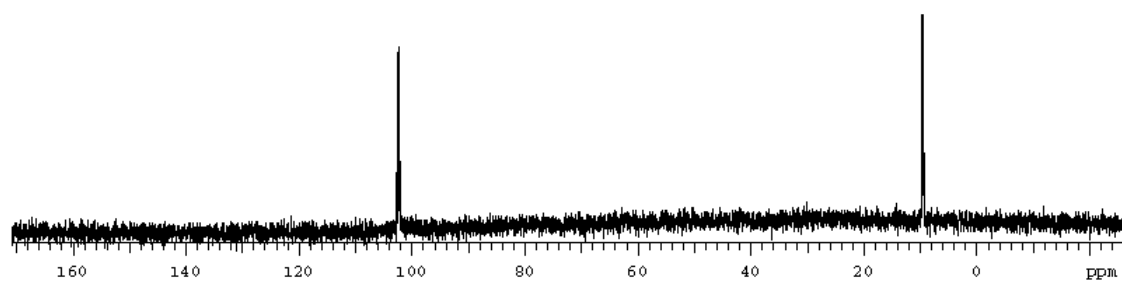
^1H at RT in d_8 -THF.



$^{13}\text{C}\{^1\text{H}\}$ at RT in d_8 -THF.



$^{29}\text{Si}\{\text{}^1\text{H}\}$ at RT in d_8 -THF.



$^{31}\text{P}\{\text{}^1\text{H}\}$ at RT in d_8 -THF.

